

DOI: 10.1002/((please add manuscript number))

Article type: Communication

3D Printable Photochromic Molecular Materials for Reversible Information Storage

Dominic J. Wales, Qun Cao, Katharina Kastner, Erno Karjalainen, Graham N. Newton, Victor Sans**

Dr. D. J. Wales

Faculty of Engineering and School of Chemistry, University of Nottingham, University Park, Nottingham, NG7 2RD, United Kingdom

Dr. Q. Cao, Dr. E. Karjalainen

Faculty of Engineering, University of Nottingham, University Park, Nottingham, NG7 2RD, United Kingdom

Dr. K. Kastner, Dr. G. N. Newton

School of Chemistry, University of Nottingham, University Park, Nottingham, NG7 2RD, United Kingdom

E-mail: graham.newton@nottingham.ac.uk

Dr. V. Sans

Faculty of Engineering, University of Nottingham, University Park, Nottingham, NG7 2RD, United Kingdom

and

GSK Carbon Neutral Laboratories, University of Nottingham, Jubilee Campus, Nottingham, NG8 2GA, United Kingdom

E-mail: victor.sanssangorin@nottingham.ac.uk

Keywords: 3D printing, polyoxometalates, poly(ionic liquids), smart materials, photochromism

Abstract: The formulation of advanced molecular materials with bespoke polymeric ionic liquid matrices that stabilize and solubilize hybrid organic-inorganic polyoxometalates and allow their processing by additive manufacturing, is effectively demonstrated. The unique photo and redox properties of nanostructured POMs are translated across the scales (from molecular design to functional materials) to yield macroscopic functional devices with reversible photochromism. These properties open a range of potential applications including reversible information storage based on controlled topological and temporal reduction/oxidation of pre-formed printed devices. This approach pushes the boundaries of

3D printing to the molecular limits, allowing us to couple the freedom of design enabled by 3D printing with the molecular tuneability of polymerizable ionic liquids and the photoactivity and orbital engineering possible with hybrid polyoxometalates.

Introduction: The next frontier in the development of advanced smart-materials is the direct translation of advanced molecular functionalities into macroscopic properties.^[1] The successful design of functional materials and devices based on molecular materials is highly complex, as it often requires the simultaneous design, creation and tailoring of the active molecular species, support materials and macroscopic geometries. Currently, there are numerous examples of smart materials that translate advanced molecular properties into the macroscopic material scale, based on responsive polymers, nanostructured materials, supramolecular recognition interactions, *etc.*^[2] Nevertheless, the translation of advanced molecular properties into the macroscopic material scale *via* 3D printing is far less exploited.

Additive manufacturing, commonly known as 3D printing, is emerging as a new set of technologies with the potential to revolutionize manufacturing by enabling the development of tailored designs, often unfeasible with traditional techniques.^[3] However, the development of advanced 3D printed functional materials, the properties of which are determined by the inclusion of molecular or nanostructured additives, is still in its infancy.^[4] Wang and He *et al.* have demonstrated the 3D printing of resins containing luminescent species into luminescent polymeric materials^[5] and Roppolo and Descrovi *et al.* have demonstrated the 3D printing of formulations containing azobenzene derivative dyes into polymeric materials which exhibit a change in Young's modulus upon laser irradiation.^[6] Furthermore, the translation of molecular motion into macroscale mechanical work in 3D printed polypseudorotaxane cubes was recently shown by Lin *et al.*, where the manufactured cubes were able to lift objects

upon solvent replacement.^[7] However, in most cases the focus has only been on the design of the properties of the molecular or nanoscale additives to be incorporated into 3D printed materials, rather than the design of the properties of both the additives and the constituent components of the 3D printed matrix material. Smart material design involves fine control of the electronic structure and chemical nature of all components, facilitating the tuneable translation of the molecular properties to a bulk printable material. Such an approach allows for the development of synergy between the constituent systems, which in turn facilitates fine tuning of the overall properties of the macroscale 3D printed material. Therefore, we proposed smart 3D printed materials, consisting of poly(ionic liquids) and photochromic polyoxometalates, wherein the tuneable properties of both components synergistically contribute to the desired functionality of the macroscale material.

Poly(ionic liquids) (PILs) are a subgroup of solid polyelectrolytes,^[8] with analogous properties to bulk ionic liquids^[9] in solution.^[10] The broad range of properties, including nanomaterial stabilization, support for catalysts, electrochemistry,^[11] *etc.* are the result of the broad range of cation/anion combinations.^[12] Furthermore, the polymer backbone of poly(ionic liquids) consists of ionic liquid monomer units, which possess a charged functional group, such as an imidazolium moiety. Therefore, through the choice of the counter anion (or cation) the synergy between the poly(ionic liquids) and additive components can be tuned. Indeed, with a near-infinite range of possible counter anions or cations, the degree to which the synergy can be tuned is very high. The possibility of 3D printing PIL type materials has been demonstrated using microstereolithography^[13] and more recently, inkjet printing.^[14]

Polyoxometalates (POMs) are a diverse class of self-assembled inorganic molecules, typically based on molecular metal oxides of W, Mo or V ions in their highest oxidation states. Their rich redox and optical properties lend them to a range of diverse applications.^[15]

^{16]} Recently, we reported the development of a new strategy to generate photosensitized molecular materials with tuneable photo-activity based on hybrid organic-inorganic POMs.^[17]

^{18]} There are examples of materials that contain photochromic polyoxometalates,^[19] however, the application of these materials can be hampered by to the inherent counter-cation dependent solubility. Furthermore, to the best of the authors' knowledge, there are no examples of 3D printed materials that transfer the tuneable molecular redox properties of polyoxometalates into macroscopic materials.

Here we demonstrate for the first time the possibility of employing additive manufacturing to generate advanced multi-material devices based on tailored synergistic combinations of PILs and hybrid organic-inorganic POMs for the development of photoactive devices. As a result, photochromic materials have been generated, which can be reversibly reduced under visible light irradiation.

Results and Discussion

Materials, Properties and Manufacturing

Initially, a tuneable formulation for the smart polymer encapsulating materials was developed. Vinyl-substituted imidazolium-based polymerizable ionic liquids (PILs) were used to stabilize novel photoactive hybrid POMs. The resultant POM@PIL mixtures were then photopolymerized layer-by-layer employing digital light processing (DLP) 3D printing.

Two ionic liquids were prepared from 3-butyl-1-vinylimidazolium bromide ([BVIM][Br]) via anion metathesis to yield one hydrophobic material based on bis(trifluoromethane)sulfonimide, [BVIM][NTf₂], and a hydrophilic system containing dicyanamide, [BVIM][N(CN)₂]. Both were liquid at room temperature, a requirement for 3D printing. Both [BVIM][N(CN)₂] and [BVIM][NTf₂] ionic liquids were found to be good solvents for the organic photoinitiator diphenyl(2,4,6-trimethylbenzoyl)phosphine oxide and crosslinking diacrylic monomers such as 1,4-butanediol diacrylate (BDA). Thus, formulations consisting of differing amounts of butyl acrylate (BuA; added to improve mechanical properties by regulating the glass transition temperature), BDA, an ionic liquid (either [BVIM][NTf₂] or [BVIM][N(CN)₂]) and the photoinitiator were prepared. These formulations were easily and reproducibly 3D printed into various geometries by DLP, as shown in the scheme in **Figure 1A**. The formulation was polymerized and 3D printed by exposure to the light from a 210 W projector lamp. A complex 3D cube comprised of repeating Schwarz P minimal surfaces^[20] (**Figure 1B**) and the sequential printing in consecutive layers of PILs with orthogonal properties (**Figure 1C**) demonstrate the potential of this technique to generate tailor-made devices. Furthermore, sequentially smaller cubes, down to ~1 cm³ with internal features on the order of ~ 1 mm, were also printed (**Figure S1**). It can be envisioned that these printable materials can find applications in flow reactors,^[21] as catalyst supports,^[22] sensors, electrolytes^[11] and membranes,^[23] amongst many others.

Location of Figure 1 (A, B &C)

Location of Figure 1 caption

Advanced Molecular Materials

Organic-inorganic hybrid photoactive POMs were incorporated into the PIL formulations to explore the potential to fabricate printed photoactive materials. We recently showed that the physical properties of POMs can be modulated at the molecular level through functionalization with organic moieties, resulting in improved photocatalytic activity under visible light irradiation.^[17, 24] The challenge here is to translate the tuneable molecular functionality of hybrid POMs across the scales, into printable materials and devices. It has been demonstrated that the properties of ionic liquids can be effectively transferred to solid-phase materials with analogous functionalities.^[10] Hence, we hypothesized that the properties of hybrid POMs would be retained in tuneable solid PIL matrices. Therefore, we chose to investigate the electrochemistry and photochemistry of a range of POMs in solution phase ILs (based on butylvinylimidazolium (BVIM) cations) and their photochemistry in the equivalent solid-phase PILs (based on the polymerized butylvinylimidazolium cations). Initially, we tested a novel hybrid organic-inorganic decyloxy(phenylphosphonato-) bifunctionalized POM, $\text{H}_6[\text{P}_2\text{W}_{17}\text{O}_{61}(\text{P}(=\text{O})\text{C}_6\text{H}_5\text{OC}_{10}\text{H}_{21})_2] \cdot 3\text{C}_4\text{H}_9\text{NO}$; {C₁₀POM}^[20] (**Figure S2**) (the number of associated molecules of *N,N*-dimethyl acetamide was estimated from the ¹H NMR), and compared its behavior to that of the recently reported benzoic acid-hybridized polyoxotungstate $\text{K}_6[\text{P}_2\text{W}_{17}\text{O}_{61}(\text{P}(=\text{O})\text{C}_6\text{H}_5\text{CO}_2\text{H})_2] \cdot 6\text{C}_4\text{H}_9\text{NO}$, {BzAcPOM} (**Figure S3**), and the parent $\text{K}_6[\text{P}_2\text{W}_{18}\text{O}_{62}]$, {P₂W₁₈} Wells-Dawson polyanion. It was found that both {P₂W₁₈} and {BzAcPOM} dissolved only in the hydrophilic [BVIM][N(CN)₂] ionic liquid. The electrochemistry of both POMs (1 wt%) in the [BVIM][N(CN)₂] IL was investigated by cyclic voltammetry **Figure 2**. The first quasi-reversible reduction process observed in the cyclic voltammogram of {BzAcPOM} occurred at -0.28 V vs. Fc/Fc⁺, a potential ~200 mV more positive than that of the parent {P₂W₁₈} anion, in agreement with our previous studies on the system.^[17, 24]

The amphiphilic nature of {C₁₀POM} ensured it was soluble in both hydrophobic and hydrophilic ionic liquids. The electrochemistry of the resulting ionic liquid solutions of the {C₁₀POM} were studied by cyclic voltammetry. The first quasi-reversible reduction process observed in the cyclic voltammogram of {C₁₀POM} in [BVIM][N(CN)₂] occurred at -0.25 V vs. Fc/Fc⁺, a potential ~50 mV more positive than the equivalent measurement in [BVIM][NTf₂] (**Figure 2**) The electrochemistry of the molecular POMs was preserved in the IL solution, which showed great promise for the translation of the molecular properties through the scales upon 3D-printing the POM@PIL inks into advanced materials.

Four combinations of POM@PIL were obtained, namely {P₂W₁₈}@[BVIM][N(CN)₂], {BzAcPOM}@[BVIM][N(CN)₂], {C₁₀POM}@[BVIM][N(CN)₂] and {C₁₀POM}@[BVIM][NTf₂]. The formulations consisted of a mixture of 80 mol% vinyl-IL monomer and 20 mol% DBA, with 1 mol% photoinitiator added. POMs were added at a loading of 1 wt%. The test strips were printed according to the DLP procedure given in the Supplementary Information. The printed devices were found to have good mechanical properties (**Figure S4**). Indeed the post-irradiation with UV light contributed to additional curing of the printed stripes, which resulted in an increase of the glass transition temperature (T_g) and the Young's modulus, even though upon extended irradiation the materials became brittle (**Figure S4**). The DLP method required that the polymerization mixture was irradiated to successively photopolymerize the layers of material. This caused the POM additives in all three samples based on the hydrophilic [BVIM][N(CN)₂] ionic liquid to undergo varying degrees of photoreduction during the 3D printing of the PIL strip, as evidenced by their blue coloration (**Figure 2**).^[16] In contrast, however, 3D printing of the hydrophobic {C₁₀POM}@[BVIM][NTf₂] resulted in a light yellow solid, indicating that the POM was still

in its oxidized state and that no appreciable photoreduction had occurred. There are two key reasons for the contrasting photoreduction properties. Firstly, the electrochemically determined first reduction (LUMO) energies of the POMs have a direct influence on their photoactivity, and consequently the ease with which they can be reduced.^[24] The positively shifted redox potentials, and therefore lower LUMO energies, of the {BzAcPOM}@[BVIM][N(CN)₂] and {C₁₀POM}@[BVIM][N(CN)₂] systems indicate that they are readily reduced. Secondly, water is known to act as a reductant upon POM photo-excitation, resulting in the transfer of one proton and one electron onto the POM, and the formation of a hydroxyl radical.^[25] The elevated concentration of water molecules in the hydrophilic PIL samples (~3.5 wt%) compared to the hydrophobic PIL samples (<1 wt%), confirmed by thermogravimetric analysis (TGA) (**Figure S5**), causes the POMs to be more readily reduced than the hydrophobic equivalent. This hypothesis was validated by exposure of {C₁₀POM} dissolved in either pure hydrophobic [BVIM][NTf₂] or pure hydrophilic [BVIM][N(CN)₂] to the printer projector light (210 W) for 72 s, an equivalent to the total exposure period during the 3D printing (**Figure S6**). The {C₁₀POM}@[BVIM][NTf₂] remained oxidized and thus remained yellow, whereas the {C₁₀POM}@[BVIM][N(CN)₂] was partially photo-reduced and thus changed color to green/blue (**Figure S6**). The photo-reduction of the POM in the hydrophilic IL suggests that water acted as the electron donor. The design of ionic liquid based monomers with tuneable properties based on the choice of anion is key to enable the dissolution and stabilization of very challenging molecules. Hybrid organic-inorganic polyoxometalates exhibit very strong solvent dependency, ranging from total insolubility in some organic media to the formation of micelles in aqueous environments and full molecular dissolution in appropriate systems.^[26] Indeed, the PILs designed and formulated for 3D printing here enabled the dissolution of up to 1 wt% of the different POMs employed, a loading that facilitates the observation of significant photochromic behavior.

Location of Figure 2

Location of Figure 2 caption

Novel Photochromic Devices

The ability of the {C₁₀POM} to remain in the oxidized form during 3D-printing of the BVimiNTf₂ strip facilitated the utilization of the printed materials as novel photochromic devices that exhibit reversible information encoding. The printed pieces of BVimiNTf₂ containing 1 wt% {C₁₀POM} were exposed to the light from the projector (Osram lamp. Power = 210W) used in the 3D-printing DLP set-up to photoreduce the {C₁₀POM} to afford blue coloration. The use of a conventional projector enabled the encoding of any shape or information into the POM@PIL strip by controlled photoreduction of the POM (**Figure 3A**). The accompanying color change upon photoreduction was observable by eye and could be monitored spectrophotometrically over time. A small strip of the {C₁₀POM}@[BVIM][NTf₂] (1 wt% {C₁₀POM}) was initially fabricated and then exposed to the projector light for either 0, 2, 5, 10, 20 or 40 min and the absorbance intensity at $\lambda_{max} = 801$ nm was recorded (**Figure 3B**). After each time exposure measurement, the sample was stored under O_{2(g)} atmosphere for 48 h to achieve oxidation back to the colorless form of {C₁₀POM}; O_{2(g)} is reduced to water by the POM, which in turn oxidizes the POM.^[27] Furthermore, it was found that the system exhibited reversibility, with several cycles of photoreduction to the blue state and subsequent oxidation back to the colorless state possible (**Figure 3C**). This demonstrates that these POM@PIL systems could be useful as novel smart rewriteable information storage materials. In addition, a small Schwarz P minimum surface cube^[20] (~1 cm³, with internal features in the order of ~1 mm) containing 1 wt% {C₁₀POM} was 3D printed and found to

retain the expected photochromism (**Figure 3D(i/ii)**), demonstrating that the photoresponsive material can be employed to fabricate complex architectures and that the molecular additive does not cause a decrease in printing resolution. In fact, the presence of {C₁₀POM} had a beneficial effect on the printing resolution (**Figure 3D(iii)**), illustrated by optical microscopy comparison of the internal features of ~1 cm³ cubes printed with and without the incorporation of {C₁₀POM} (**Figure S7**).

Location of Figure 3 (A, B, C & D)

Location of Figure 3 caption

Conclusions

Additive manufacturing techniques allow for transfer across the scales of properties of advanced molecular moieties into smart advanced materials. Herein, it has been demonstrated that synergy between the molecular photo- and electrochemical properties of hybrid organic-inorganic polyoxometalates and the molecular properties of the anions of polymeric ionic liquid matrices can be tuned to give rise to smart materials that show great potential for reversible information encoding, storage and retrieval. Initially the hybrid POM ({BzAcPOM}), previously reported by our group as a POM which is photoactive under visible light irradiation, was found to only be soluble in the [BVIM][N(CN)₂] ionic liquid. However, more crucially, cyclic voltammetry experiments demonstrated that the electrochemistry of the hybrid {BzAcPOM} was maintained upon dissolution in the ionic liquid. However, another visible light photoactive hybrid organic-inorganic POM that would dissolve in both the hydrophilic [BVIM][N(CN)₂] and hydrophobic BVimiNTf₂ ionic liquids was required. Thus, the novel amphiphilic organic-inorganic hybrid {C₁₀POM} was synthesized and it was found to be soluble in both ionic liquids. Cyclic voltammetry

experiments revealed that the electrochemistry of this POM was also maintained in the ionic liquids. However, 3D printing of the hydrophilic $\{C_{10}POM\}@[BVIM][N(CN)_2]$ composition afforded a blue solid, indicating that the $\{C_{10}POM\}$ had been photoreduced. This was attributed to the presence of water within the hydrophilic 3D printed matrix acting as a sacrificial oxidant leading to the reduction of the POMs. For the generation of 3D printed materials for data storage and retrieval the material ideally should start in the '0' or 'off' binary state (in this case 'yellow') and through on-demand photoreduction, access the '1' or 'on' binary state (in this case 'blue'). Thus, the $\{C_{10}POM\}@[BVIM][N(CN)_2]$ composition was unsuitable. However, upon 3D printing the hydrophobic $\{C_{10}POM\}@BVimiNTf_2$ composition a light-yellow solid was afforded, indicating the $\{C_{10}POM\}$ had not been reduced during the 3D printing and thus was still in the '0' or 'off' state, ready for on-demand photoreduction. Controlled topological and temporal photoreduction to the '1' or 'on' state was achieved and it was subsequently shown that the $\{C_{10}POM\}$ could be oxidized back to the '0' or 'off' state. This could be repeated for several cycles. This was achieved by smart design of the synergy between the hydrophobic property of the NTf_2 anion of the PIL matrix and the properties of the organic-inorganic hybrid $\{C_{10}POM\}$.

Overall, the unique photo and redox properties of molecularly engineered nanostructured POMs were translated across the scales to yield macroscopic functional devices with reversible photochromism. These materials have a range of applications including reversible information storage based on controlled topological and temporal reduction/oxidation of pre-formed printed devices. This approach allows coupling the freedom of design associated to 3D printing with the molecular tuneability of polymerizable ionic liquids and the band gap engineering possible with hybrid polyoxometalates.

Experimental Section

General Experimental Information: Unless otherwise stated, all reagents were purchased from Sigma-Aldrich and used without further purification. 1,4-butanediol diacrylate (BDA) (90%) and 1-vinylimidazole were used after purification by passing through a short column of basic alumina (aluminum oxide). The 3D printer used in this study was a LittleRP 3D printer. An Acer P1500 projector was used as the 3D printer light source and it was equipped with an OSRAM Lamp (210 W). UV-Vis spectra were collected using an Agilent Cary 5000 UV-Vis-NIR spectrophotometer. FT-IR spectra were collected on a Bruker Alpha fitted with a Platinum ATR module. ^1H NMR spectra were recorded on a Bruker AVX400 (400 MHz) spectrometer at ambient temperature. ^{13}C NMR spectra were recorded on a Bruker AVX400 (101 MHz) spectrometer at ambient temperature. ^{19}F NMR spectra were recorded on a Bruker AVX400 (376 MHz) spectrometer at ambient temperature. ^{31}P NMR { ^1H decoupled} spectra were recorded on a Bruker AVX400 (162 MHz) spectrometer at ambient temperature. High resolution GC-MS mass spectra were recorded using a JEOL AccuTOF GCX mass spectrometer connected to an Agilent 7890B gas chromatograph. The MS ion source conditions were as follows: electron ionization mode, ionization energy: 70eV and temperature: 150 °C, with a mass range between 50 – 600 Da with mass calibration by PFTBA. The chromatography conditions were as follows: the GC column was a Thermo Scientific TraceGold TG_POLAR (30m x 0.25mm x 25um) with a column temperature program of 40 °C (4min) to 260 °C (5min) @ 10 °C min⁻¹, helium carrier gas, an inlet temperature of 200°C and a transfer line temperature of 230 °C. High resolution electrospray ionization (ESI) mass spectra were recorded using a Bruker MicroTOF mass spectrometer in either positive or negative ionization mode. MALDI mas spectra were collected in negative ionization mode using a Bruker Ultraflex mass spectrometer and *trans*-2-[3-(4-tert-Butylphenyl)-2-methyl-2-propenylidene]malononitrile (DCTB) as the matrix. Thermal gravimetric analysis was performed on a TA Instruments TGA Q500 analyzer. Samples for

TGA analysis were heated in an inert atmosphere up to 800 °C with a heating rate of 10 °C min⁻¹.

Synthesis of ionic liquids, organic ligands, POMs and inorganic-organic hybrid POMs: Full synthetic details and characterization data are given in the Supplementary Information.

Process for stereolithography 3D printing imidazolium PIL networks: All of the 3D printed imidazolium ionic liquid network pieces were fabricated following a similar procedure (**Scheme S1**) and the construction of 24 mm x 16 mm x 0.5 mm, poly(BDA-co-BVimiTf₂N) 3D test specimen (**Figure S8**) with 80 mol% BVimiNTf₂ ionic liquid is given as an example. Stereolithography fabrication began by slicing a 3D computer aided design (CAD) model into individual images for projecting onto the photo curable ink. Additive manufacturing software, Creation Workshop RC36, was used to create slices of a desired thickness (50 µm layer⁻¹), control the projection time of the images by the projector, and the movement of the build plate. A LittleRP FlexVat was filled with premixed PIL ink which contains 80 mol% BVimiNTf₂ (80 mmol, 34.4832 g), 20 mol% 1,4-butanediol diacrylate (20 mmol, 3.9644 g) and 1 mol% diphenyl(2,4,6-trimethylbenzoyl)phosphine oxide (1 mmol, 0.3484 g). Then the build plate was lowered into the ink against the transparent Teflon film of the FlexVat. The Creation Workshop RC36 then controled the projector to show a black background with white images of each of the layers which were to be photo cured. The UV light passed from the projector lamp and mirror to the transparent Teflon film of the FlexVat. Each layer (50 µm) was cured for 8 s. After 8 s, the projector showed black background – negligible light was projected into the photocurable ink while the build plate lifted up by 50 µm. Then the Creation Workshop RC36 software loaded the image of the next layer and turned “on” the projector by showing the next white color image. This process was repeated until the object

was completely fabricated. After the object was fabricated, the object was isolated and washed with isopropyl alcohol (IPA) to remove any uncured ink. Then the object was dried in the dark at room temperature overnight. Note: For the test of photocoloration effect, one weight percent (1 wt%) of POM (polyoxometalate) was added to the photo curable ink and stirred for 30 min in the dark at room temperature before beginning the 3D printing process.

Process for Testing C10POM Photocoloration Effect: When a specimen containing C10POM was irradiated by projector light (2 min), a color change from light-yellow to blueish-green occurred, which was visible with the naked eye. If a blueish-green specimen was stored in the dark in the presence of O₂, the specimen would change color to pale yellow/green after 48 hours (no color reversion took place in an O₂ free atmosphere).

UV-Vis absorbance measurements of printed pieces: For collection of the UV-vis absorbance spectra of the 3D printed specimen, before and after irradiation with projector light, the specimen was first affixed to a metal holder (**Figure S9a**), placed in the FlexVat ink tank (containing no ink) and exposed to projector light for a determined fixed amount of time (**Figure S9b**), then a UV-vis spectrum of this specimen was collected using Cary 5000 UV-Vis-NIR spectrophotometer. After measurement, the sample was stored under O₂ atmosphere for 48 h, then another UV-Vis spectrum of the sample was collected.

Cyclic voltammetry experiments: Cyclic voltammetry (CV) experiments in ionic liquids were performed (no supporting electrolyte) using a CHI Instruments electrochemical workstation equipped with a glassy carbon (d = 3 mm) working electrode, a Pt wire counter electrode and a Ag wire pseudo-reference electrode (placed in an Eppendorf™ pipette tip to reduce the surface area). All potentials with ferrocene as internal reference are quoted relative to NHE.

All solutions were purged with N₂ for at least 10 min to remove O₂. Measurements were performed at room temperature (~21 °C), at a scan rate of 100 mV s⁻¹ and with a sampling interval of 1 x 10⁻³ V.

Supporting Information

Supporting Information (Scheme S1, Figures S1-9 and full synthetic details and characterization data for the ionic liquids, organic ligands, POMs and inorganic-organic POMs) is available from the Wiley Online Library or from the author.

Acknowledgements

The authors thank the University of Nottingham (Dean Prize of Engineering, Nottingham Research Fellowship and the Advanced Molecular Materials and Antimicrobial Resistance Research Priority Areas) for funding. The Leverhulme Trust is gratefully acknowledged for funding (RPG-2016-442). KK thanks the Deutscher Akademischer Austausch Dienst (DAAD). EK acknowledges the Finnish Cultural Foundation (Suomen Kulttuurirahasto) for personal funding. DJW would like to thank Dr J. M. Cameron for assistance in preparation of [BVIM][N(CN)₂] and Mr S. Amin for assistance in preparation with {C₁₀POM} and with MALDI mass spectrometry.

Received: ((will be filled in by the editorial staff))

Revised: ((will be filled in by the editorial staff))

Published online: ((will be filled in by the editorial staff))

References

- [1] A. S. Lubbe, T. van Leeuwen, S. J. Wezenberg, B. L. Feringa, *Tetrahedron* **2017**, *73*, 4837; M. B. Avinash, T. Govindaraju, *Acc. Chem. Res.* **2018**.
- [2] J. Hu, S. Liu, *Macromolecules* **2010**, *43*, 8315; A. Harada, R. Kobayashi, Y. Takashima, A. Hashidzume, H. Yamaguchi, *Nat. Chem.* **2011**, *3*, 34.
- [3] I. Gibson, D. W. Rosen, B. Stucker, *Additive Manufacturing Technologies: Rapid Prototyping to Direct Digital Manufacturing*, Springer-Verlag Berlin, Berlin 2010.
- [4] E. García-Tuñón, S. Barg, J. Franco, R. Bell, S. Eslava, E. D'Elia, R. C. Maher, F. Guitian, E. Saiz, *Adv. Mater.* **2015**, *27*, 1688; M. Zarek, M. Layani, I. Cooperstein, E. Sachyani, D. Cohn, S. Magdassi, *Adv. Mater.* **2016**, *28*, 4449; R. D. Farahani, M. Dubé, D. Therriault, *Adv. Mater.* **2016**, *28*, 5794; E. Fantino, A. Chiappone, I. Roppolo, D. Manfredi, R. Bongiovanni, C. F. Pirri, F. Calignano, *Adv. Mater.* **2016**, *28*, 3712; H. Yang, W. R. Leow, T. Wang, J. Wang, J. Yu, K. He, D. Qi, C. Wan, X. Chen, *Adv. Mater.* **2017**, *29*, 1701627.
- [5] F. Wang, Y. Chong, F. Wang, C. He, *J. Appl. Polym. Sci.* **2017**, *134*, 44988.
- [6] I. Roppolo, A. Chiappone, A. Angelini, S. Stassi, F. Frascella, C. F. Pirri, C. Ricciardi, E. Descrovi, *Mater. Horiz.* **2017**, *4*, 396.

- [7] Q. Lin, X. Hou, C. Ke, *Angew. Chem.* **2017**, *129*, 4523; *Angew. Chem. Int. Ed.* **2017**, *56*, 4452.
- [8] D. Mecerreyes, *Prog. Polym. Sci.* **2011**, *36*, 1629.
- [9] J. Dupont, *J. Braz. Chem. Soc.* **2004**, *15*, 341.
- [10] V. Sans, N. Karbass, M. I. Burguete, V. Compañ, E. García-Verdugo, S. V. Luis, M. Pawlak, *Chem. Eur. J.* **2011**, *17*, 1894.
- [11] M. Armand, F. Endres, D. R. MacFarlane, H. Ohno, B. Scrosati, *Nat. Mater.* **2009**, *8*, 621.
- [12] W. Qian, J. Texter, F. Yan, *Chem. Soc. Rev.* **2017**, *46*, 1124.
- [13] A. R. Schultz, P. M. Lambert, N. A. Chartrain, D. M. Ruohoniemi, Z. Zhang, C. Jangu, M. Zhang, C. B. Williams, T. E. Long, *ACS Macro Letters* **2014**, *3*, 1205.
- [14] E. Karjalainen, D. J. Wales, D. H. A. T. Gunasekera, J. Dupont, P. Licence, R. D. Wildman, V. Sans, *ACS Sustainable Chem. Eng.* **2018**, DOI: 10.1021/acssuschemeng.7b04279.
- [15] T. Yamase, *Chem. Rev.* **1998**, *98*, 307.
- [16] D. L. Long, E. Burkholder, L. Cronin, *Chem. Soc. Rev.* **2007**, *36*, 105.
- [17] J. M. Cameron, S. Fujimoto, K. Kastner, R.-J. Wei, D. Robinson, V. Sans, G. N. Newton, H. H. Oshio, *Chem. Eur. J.* **2017**, *23*, 47.
- [18] J. M. Cameron, D. J. Wales, G. N. Newton, *Dalton Trans.* **2018**, DOI: 10.1039/C8DT00400E.
- [19] T. He, J. Yao, *Prog. Mater. Sci.* **2006**, *51*, 810.
- [20] The Schwarz P Surface Cube by moczys on Thingiverse (Published on September 12, 2015), <http://www.thingiverse.com/thing:1011576>, (accessed: April 2018).
- [21] O. Okafor, A. Weilhard, J. A. Fernandes, E. Karjalainen, R. Goodridge, V. Sans, *React. Chem. Eng.* **2017**, *2*, 129; V. Sans, F. Gelat, M. I. Burguete, E. Garcia-Verdugo, S. V. Luis, *Catal. Today* **2012**, *196*, 137; E. Peris, O. Okafor, E. Kulcinskaja, R. Goodridge, S. V. Luis, E. Garcia-Verdugo, E. O'Reilly, V. Sans, *Green Chem.* **2017**, *19*, 5345.
- [22] P. J. Kitson, M. H. Rosnes, V. Sans, V. Dragone, L. Cronin, *Lab Chip* **2012**, *12*, 3267.
- [23] J.-K. Sun, H.-J. Lin, W.-Y. Zhang, M.-R. Gao, M. Antonietti, J. Yuan, *Mater. Horiz.* **2017**, *4*, 681.
- [24] S. Fujimoto, J. M. Cameron, R.-J. Wei, K. Kastner, D. Robinson, V. Sans, G. N. Newton, H. Oshio, *Inorg. Chem.* **2017**, *56*, 12169.
- [25] G. Bernardini, A. G. Wedd, C. Zhao, A. M. Bond, *Proc. Natl. Acad. Sci.* **2012**, *109*, 11552.
- [26] K. Kastner, A. J. Kibler, E. Karjalainen, J. A. Fernandes, V. Sans, G. N. Newton, *J. Mater. Chem. A* **2017**, *5*, 11577.
- [27] E. Papaconstantinou, A. Hiskia, in *Polyoxometalate Molecular Science*, (Eds: J. J. Borrás-Almenar, E. Coronado, A. Müller, M. Pope), Kluwer Academic Publishers, 2003, 381.

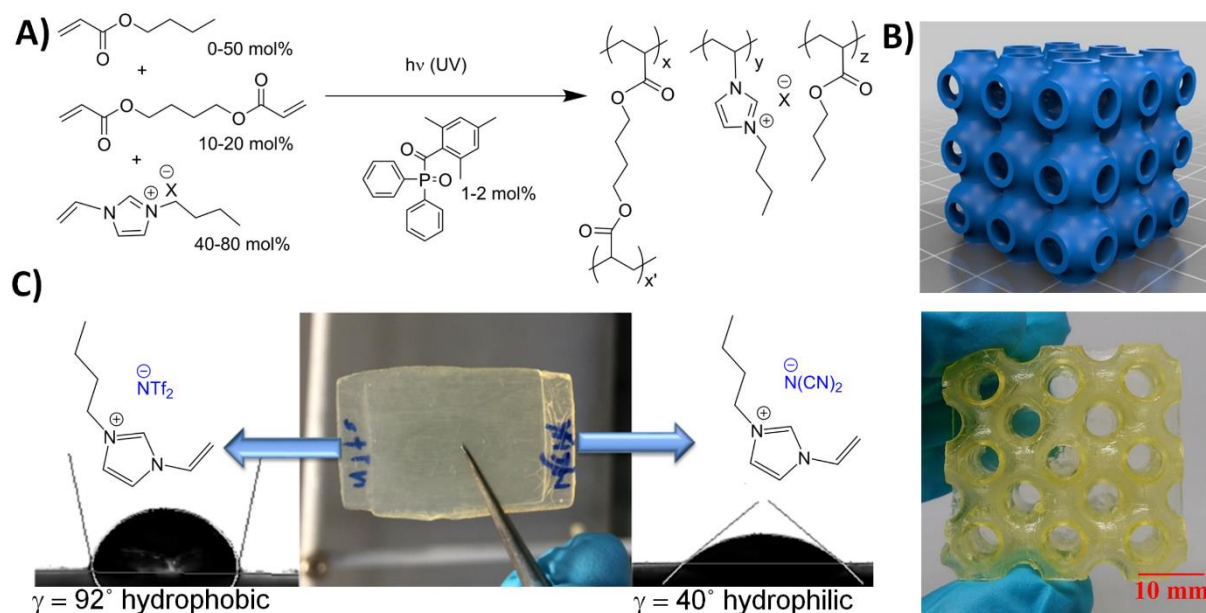


Figure 1. A) Compositions of the 3D printing formulation containing PILs explored in this work. B) Example of a PIL-based 3D printed complex geometry, in this case a cube consisting of a repeating Schwarz P minimal surface.^[20] C) Multifunctional printing of hydrophilic and hydrophobic PILs in consecutive layers. Image in upper part of (B): Reproduced with permission.^[20] Copyright 2015, Seth Moczylowski. Permission from Seth Moczylowski was also granted for the reproduction of the structure, as shown in the lower panel.

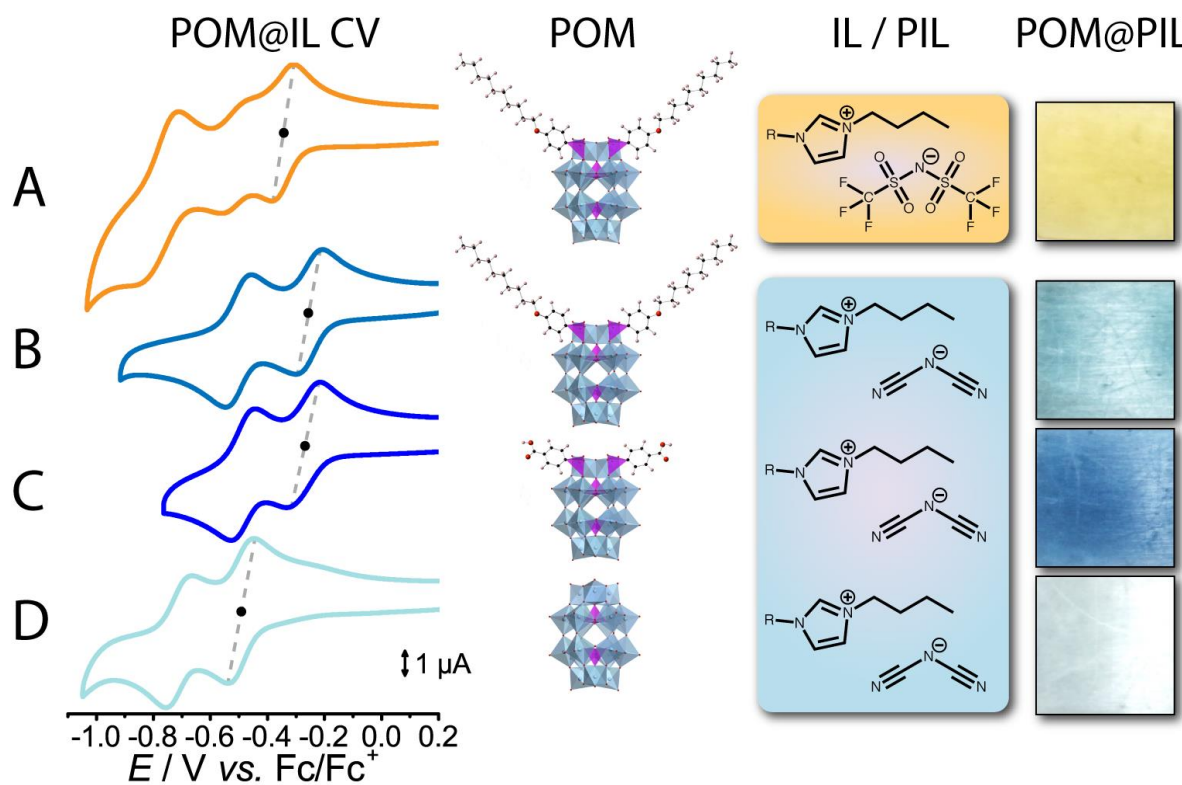


Figure 2. Tuneable hybrid organic-inorganic POMs preserve their redox properties in ionic liquids. Stabilization/solubility of the POMs is dependent on the IL and redox properties are dependent on the PIL-POM composition. For compositions A and B the POM is $\{C_{10}POM\}$, for composition C the POM is $\{BzAcPOM\}$ and for composition D the POM is $\{P_2W_{18}\}$. In all cases R = vinyl moiety.

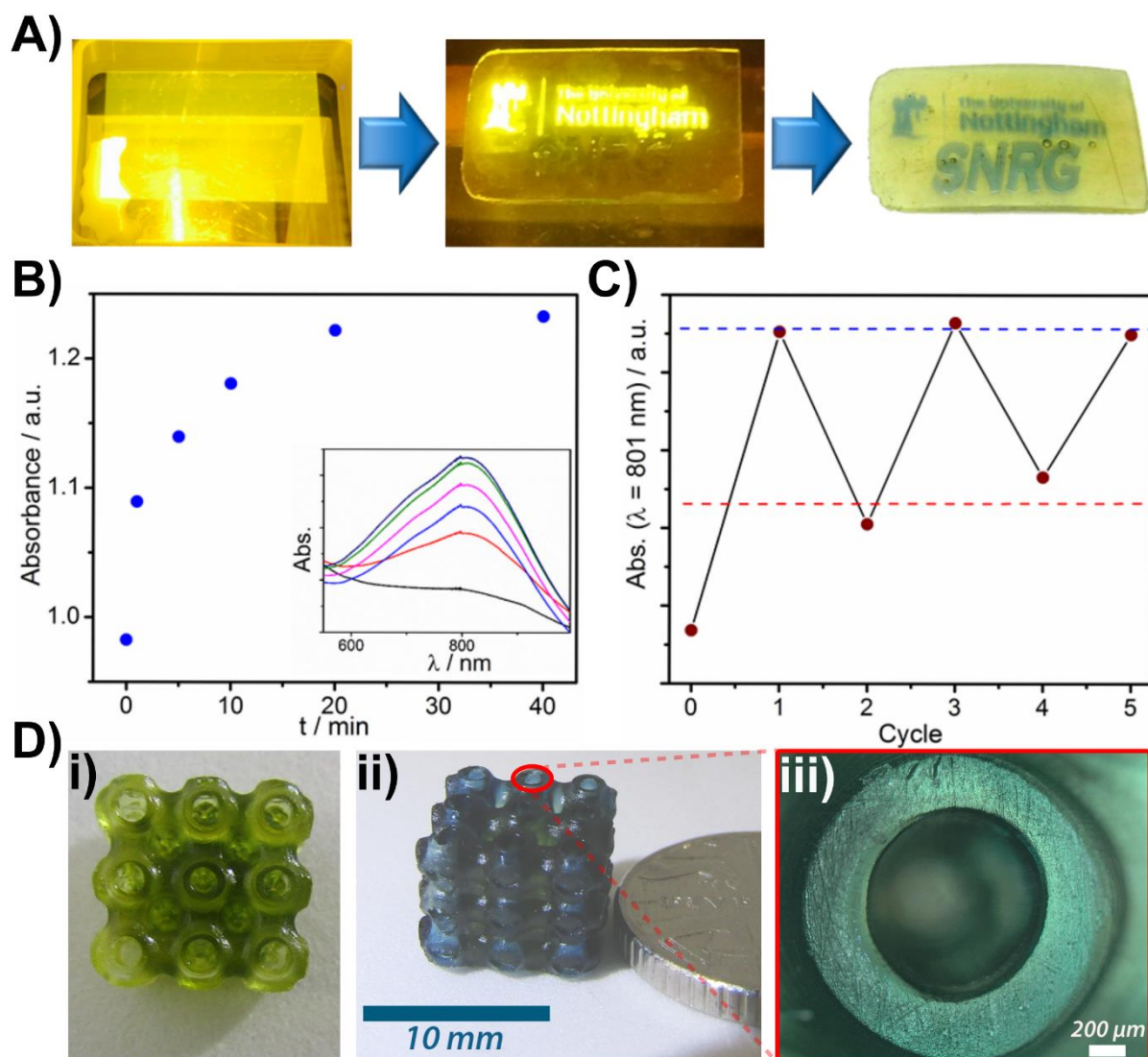


Figure 3. A) Controlled topological and temporal photoreduction of the $\text{C}_{10}\text{POM@BVimiNTf}_2$ material with visible light from a projector (Osram lamp, 210 W) to encode information. B) Increase in absorption at $\lambda_{\text{max}} = 801 \text{ nm}$ due to photoreduction of the encapsulated $\{\text{C}_{10}\text{POM}\}$ upon exposure to the project light over time and (inset) shows the corresponding UV-visible spectra. C) Information encoded by photoreduction could be erased and reprinted several times, as evidenced by change in the absorbance intensity at $\lambda_{\text{max}} = 801 \text{ nm}$ upon cycles of photoreduction (encoding) and oxidation (erasure). For odd number cycles the values of absorbance intensity were recorded after photoreduction and for even number cycles the values of absorbance intensity were recorded after oxidation with $\text{O}_{2(\text{g})}$ for 48 h. D) (i) 1 cm^3 Schwartz P Surface Cube^[20] printed with $\text{C}_{10}\text{POM@BVimiNTf}_2$ as printed; (ii) after 20 minutes UV irradiation; and (iii) optical micrograph highlighting printing resolution.

Novel reversible photochromic materials consisting of bespoke poly(ionic liquid) matrices and hybrid organic-inorganic polyoxometalates are presented. The unique photoredox properties of nanostructured polyoxometalates are translated across the size scales to yield macroscopic functional photochromic devices. The freedom afforded by 3D printing is coupled with the molecular tuneability of poly(ionic liquids) and the photoactivity and orbital engineering enabled by hybrid polyoxometalates.

Dominic J. Wales, Qun Cao, Katharina Kastner, Erno Karjalainen, Graham N. Newton*, Victor Sans*

3D Printable Photochromic Molecular Materials for Reversible Information Storage

